Fusion Engineering and Design 219 (2025) 115244

Contents lists available at ScienceDirect

Fusion Engineering and Design

journal homepage: www.elsevier.com/locate/fusengdes

# Achieving high amplifications in a cw-driven optical cavity relevant for photoneutralization of negative ion beams

R. Friedl [a,*], R. Borkenhagen [a,1], U. Fantz [a,b]

[a] AG Experimentelle Plasmaphysik, Universität Augsburg, Augsburg, 86135, Germany
[b] Max–Planck-Institut für Plasmaphysik, Boltzmannstr. 2, Garching, 85748, Germany

ARTICLE INFO

*Keywords:*
Neutral beam heating
Negative ion beam
Photo-detachment
Laser neutralizer
Resonant cavity
Cavity folding

ABSTRACT

In order to overcome the drawback of the limited neutralization efficiency of a gas neutralizer, laser neutralization is discussed for negative ion based neutral beam injection systems for future fusion devices. Those could easily deliver neutralization efficiencies far beyond the 60% constraint of conventional systems, in principle only limited by the provided optical power. For fusion-relevant ion beams, optical powers beyond tens of MW would be required, which poses the challenge of reliably providing such high powers in cw operation. Measures to amplify the optical power are thus mandatory and high-finesse optical cavities wrapped around the ion beam can be applied for this purpose. The target is to reduce the initially required laser power by three to four orders of magnitude and maintain stable coupling of the laser and the enhancement cavity in resonance. In order to confirm that such high amplifications can be reliably obtained in cw, an independent optical test bench was set up. The setup proved that using a two-fold feedback system (Pound–Drever–Hall locking scheme), stable resonance locking of laser and cavity for more than an hour is feasible. Furthermore, amplifications of 7'000 could be achieved experimentally, reaching in-cavity powers in the range of several kW, driven by only 240 mW input power. Approaches to integrate such a laser neutralizer setup at the negative ion beam facility Batman Upgrade and options for cavity folding are discussed in terms of the achievable neutralized fraction of the ion beam.

## 1. Photo-detachment neutralization

The ITER neutral beam injection (NBI) system is based on negative hydrogen ions and relies on a gas neutralizer, in which the additional electron of the negative ions is stripped by collisions with a gas target. The efficiency of this mechanism is, however, below 60% leading to a limited overall efficiency of the NBI of about 26% [1]. Hence, alternative concepts for the neutralization of the negative ion beam represent a valuable opportunity to increase the wall-plug efficiency of future devices. Here, the photo-detachment (PD) process could be applied [2,3], as illustrated in Fig. 1(a): A high-power photon field, typically a laser, crosses the ion beam where in the interaction region the electron is detached from the negative ion. It is shown that for a 1 MeV negative deuterium ion beam with ITER-like current, optical powers beyond tens of MW are necessary [4–7]. This arises from the rather small cross section of the PD process [8], which, however, also means negligible consumption of the optical power by the neutralization itself. This has two important implications:

1. The size of the negative ion beam within the PD neutralization region ($w \times h$ in Fig. 1(a)) can be large in laser beam direction ($h$). Perpendicular to it ($w$), the ion beam is limited by the dimension of the laser beam in order to ensure full coverage. Since typical laser diameters are in the range of cm, the ion beam should be designed with a high aspect ratio ($\sim$ cm $\times$ m), giving rise to the term *beam sheet*.
2. The radiation can be re-used several times. This opens up the field of re-circulating the laser within the neutralization region, which is equivalent to an *amplification* of the initial input power.

Assuming full coverage of the ion beam by the laser beam, the correlation between optical power $P$ and neutralization efficiency $f$ follows [2,3,6]:

$$f = 1 - \exp\left(-\frac{P\,\sigma_{\mathrm{PD}}}{E_{\mathrm{ph}}\,w\,v_{\mathrm{D^-}}}\right), \tag{1}$$

* Corresponding author.
*E-mail address:* roland.friedl@physik.uni-augsburg.de (R. Friedl).
[1] Currently at Experimentalphysik II, Universität Augsburg, 86135 Augsburg, Germany.

https://doi.org/10.1016/j.fusengdes.2025.115244
Received 14 January 2025; Received in revised form 9 May 2025; Accepted 30 May 2025
Available online 27 June 2025

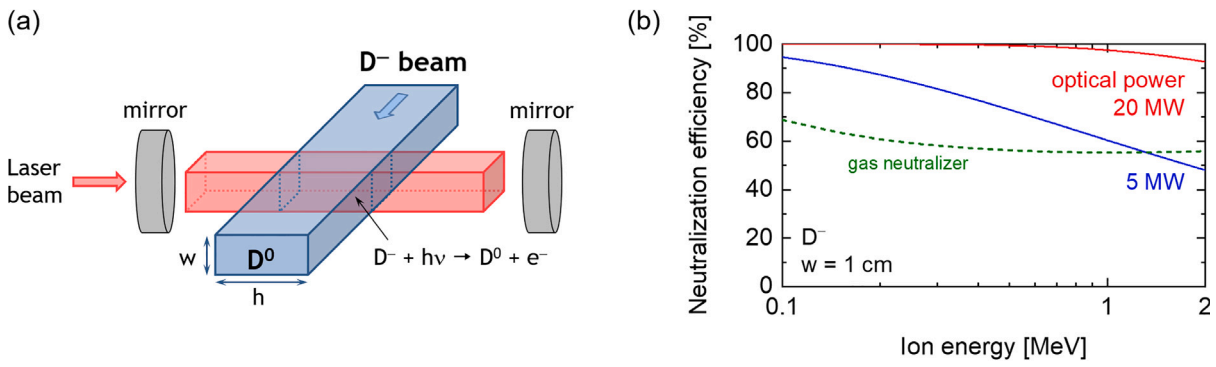


**Fig. 1.** (a) Schematic of the principle of a neutralizer based on the photo-detachment process. (b) Neutralization efficiency of gas [9] and laser neutralization, the latter calculated after Eq. (1) [2,3,6] for different total optical powers and the following parameters: $\sigma_{PD} = 3.5 \times 10^{-21}$ m$^2$ [8] at 1064 nm, and $w = 1$ cm as defined in part (a).

with the PD cross section $\sigma_{PD}$, the energy of the laser photons $E_{ph}$, and the velocity of the negative ions $v_{D^-} = \sqrt{2eU_{tot}/m_{D^-}}$ accelerated by the total potential $U_{tot}$. As discussed above, $f$ is independent of $h$ and larger widths $w$ of the laser (and ion) beam lead to lower neutralization efficiencies due to a lower optical power density at the neutralization region. Furthermore, the dependency of the ion velocity arises from the decreasing interaction time between radiation field and ions, while increasing the photon energy decreases the photon rate $P/E_{ph}$ (at constant optical power).[2] Taking further recycling of the laser power into account, $P$ can be substituted by $P_{in}\Gamma$, with the initial input power $P_{in}$ and the amplification $\Gamma$.

Achievable neutralization efficiencies calculated after Eq. (1) are shown in Fig. 1(b) and compared to the one of a gas neutralizer [9]. Using an ion beam width $w$ of 1 cm, completely covered by the laser beam, and a total (possibly re-circulated) optical power of 20 MW, the neutralization efficiency for a $D^-$ beam energy of 1 MeV is higher than 97.5%. For large fusion-relevant ion beams, several of such laser beams would be required to cover the entire beam, as for instance shown in [7].

To deliver such high optical powers, several concepts exist. Inoue [4] described a system in which an array of a huge number of high-power laser diode stacks directly illuminates the ion beam (direct drive), which was successfully applied to $H^-$ beams on much smaller scales [10]. Popov [11] uses a non-resonant adiabatic photon trap to obtain a comparable high-power photon field in the neutralization region. Further ideas rely on optical cavities, i.e. high-reflective mirrors wrapped around the ion beam [3]. Fassina [12] proposes to use the RING concept, in which the second harmonic of a pulsed seed laser is trapped in the cavity. A very efficient way of multiplying the laser power is by resonant systems. Kovari [6] describes the single cavity concept, in which the ion beam is introduced in the actual laser cavity. Thin-disc lasers mounted on one of the cavity mirrors are suggested for such a system. In contrast, Chaibi [5] proposed Fabry–Perot (FP) cavities as enhancement cavities to amplify the injected laser radiation, as also depicted in Fig. 1(a). FP cavities are most advanced in the context of amplification and have the prospect of reducing the initially required laser power by three to four orders of magnitude. This has the advantage to bring the required input laser power down to the kW range, which is commercially available. However, the challenge for this concept is to keep the input laser and the cavity continuously in resonance, for which sophisticated feedback systems need to be applied. Bresteau et al. [13] have successfully demonstrated neutralization of a nA-scale $H^-$ beam at 1.2 keV using a three-mirror resonant cavity: neutralization efficiencies of larger than 50% could be obtained with an input power of 24 W and an amplification of 583 (reaching intra-cavity powers of 14 kW). The amplification factor depended on the input power and reached 900 in maximum at a medium input power of 10 W. However, amplifications in the range of several thousands and long-time stability were still to be demonstrated. In view of future fusion relevant intra-cavity powers (MWs), thermal loads at the mirrors will become another issue and possible deformations of the substrate will additionally have to be accounted for, as pointed out by Fiorucci et al. [14].

In order to confirm that amplifications above $10^3$ can be reliably obtained, an independent optical test bench based on a linear FP cavity (two mirrors) was set up [15]. It aims at fulfilling a stable (1 h) coupling of a cw laser with moderate power to a high-finesse enhancement cavity and at achieving amplifications up to $10^4$.

## 2. Optical setup and feedback system

Coupling of a laser with a cavity is often applied in the area of laser diagnostics, a prominent example being the cavity ring-down spectroscopy (CRDS) [16]. Those systems, however, typically rely on pulsed operation, do not need to be driven in resonance and are thus considerably less complex compared to the envisaged resonant steady-state operation in the current context.

In order to fulfil the requirement of a high cw amplification, the laser field modes have to be adapted to the envisaged propagation within the resonator:

- The transversal mode describes the geometric distribution of the laser field perpendicular to the propagation direction. The highest power density is given by the so-called fundamental mode, i.e. the $TEM_{00}$ mode, also known as Gaussian mode. In order to achieve this, two high-quality lenses are applied to adapt the laser beam profile to a Gaussian propagation within the cavity. This is called optical *mode matching*.
- The longitudinal mode describes the relation of the laser wavelength and the cavity length, i.e. the distance between the mirrors. In resonance (and when mode matching is achieved, see above), the laser field is superimposed by itself and highest amplifications can be obtained. In order to achieve this, the laser wavelength is continuously adapted to the cavity length by using a sophisticated feedback system. This so-called *mode locking* is done via the Pound–Drever–Hall (PDH) scheme [17] consisting of several optical and electrical components as shown in the following.

The applied setup is shown in Fig. 2, mounted on a vibration isolated optical table of 1.2 × 2.4 m. The laser is a cw DPSS Nd:YAG laser driven at its fundamental wavelength of 1064 nm with 8 W maximal emission power (MOPA) and a minimal linewidth of 1 kHz. The linear two-mirror resonator consists of two concave mirrors with 1 m curvature radius and in-house measured reflectivity of $R^*$ = 99.995%

[2] The overall dependency of $f$ from the laser wavelength $\lambda$, given by the term $\sigma_{PD}(\lambda)/E_{ph}(\lambda)$ is illustrated in [6], showing a maximum around 1050 nm, close to the Nd:YAG fundamental wavelength of 1064 nm.

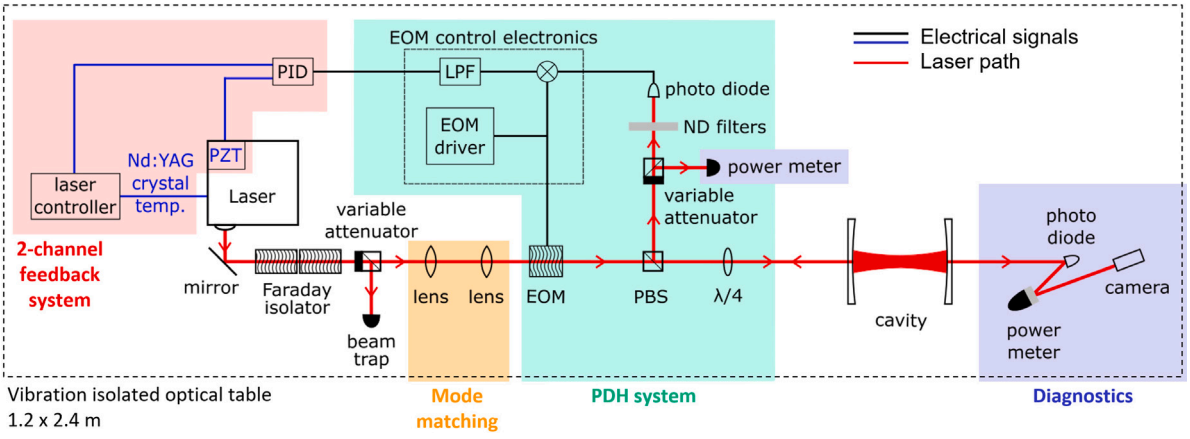


**Fig. 2.** Optical and electrical setup for the test bench to investigate the cw coupling of an external laser and an enhancement cavity in terms of stability and amplification.

and transmission $T = 39$ ppm. The mirror distance is 1.1 m, which gives a free spectral range (FSR) of $\Delta\lambda = 136$ MHz and a cavity linewidth of $\delta\lambda = 2.2$ kHz. This leads to a maximum amplification by the resonator of 15'600, if any losses are neglected.

The laser radiation is reflected by an adjustment mirror and is led through a double stage Faraday isolator that prevents back-reflected light from re-entering the laser head. Via a variable beam attenuator, the optical power from the laser (driven at the nominal value of 8 W) can be adjusted without losing the characteristic parameters of the laser beam like beam width, divergence and direction. Typically, powers of below 1 W are used for the current studies in order to reduce the power load on the cavity mirror surfaces at high amplifications. Beam shaping, i.e. mode matching, is achieved via the subsequent high-quality lenses. The electro-optical phase modulator (EOM) modulates the laser frequency, creating sidebands in the frequency spectrum. This is required for the Pound–Drever–Hall (PDH) locking technique described below. According to the horizontal polarization of the laser, the following polarizing beam splitter (PBS) transmits the laser light in forward direction. With the subsequent $\lambda/4$ waveplate the linearly polarized light is converted to circular polarization. Once mode matching and locking are achieved the laser light is coupled into the optical cavity.

Even when the laser frequency $\omega_{laser}$ is locked to the resonance frequency $\omega_{cavity}$ of the cavity, at least the modulated sidebands are reflected back from the entrance cavity mirror and are converted to vertically polarized light at the $\lambda/4$ waveplate. The beam splitter now directs the light towards a photo detector required for the PDH locking. Since without mode lock the full laser power is reflected by the cavity, the laser needs to be attenuated before irradiating the photo diode to prevent damage. This is performed by another attenuator combined with neutral density (ND) filters. Since most of the laser power is deflected by the attenuator, this side arm can be used to monitor the laser power with a calibrated power meter (Thorlabs PM100D with S314C thermal detector, 10 mW – 40 W, ±3% absolute accuracy).

The electronics for the PDH feedback loop starts with the detected signal from the photo diode that is transferred to the control electronics for the EOM. Here it is mixed with the phase-shifted reference signal from the driver and passed through a low pass filter (LPF). The output signal depends on the difference between the cavity resonance frequency and the laser frequency, having different signs for $\omega_{laser} < \omega_{cavity}$ and $\omega_{laser} > \omega_{cavity}$. It can thus be used as the error signal for a PID controller, which drives the frequency variation of the laser. For the employed laser system this can be done by two separate channels: a fast channel (bandwidth ≈1 kHz, 1.5 MHz/V wavelength tuning, 300 MHz tuning range) via a piezo crystal (PZT) mounted at the Nd:YAG crystal inside the laser head, and a slow channel (≈1 Hz bandwidth, −3 GHz/K wavelength tuning, 30 GHz tuning range) via the temperature of the Nd:YAG crystal (applied through the temperature regulation system of the laser control electronics). In this way the laser frequency can be shifted to the cavity resonance and will continuously follow it, compensating any mechanical vibrations (fast channel, 'PZT channel') or thermal drifts (slow channel, 'thermal channel') of the cavity.

The coupling is monitored by several diagnostics, mounted behind the resonator. A photodiode records the transmitted light with high temporal resolution while a calibrated power meter with slower response (Newport 843-R with 818-UV/DB photodetector, 0.1 nW–50 mW, ± 4% absolute accuracy) is used in locked state to measure the absolute transmitted power $P_{out}$. A camera is applied to observe the geometric distribution of the laser field within the resonator, i.e. the transversal mode. Due to reflective surfaces at the photo diode and the power meter, all three diagnostics can be applied simultaneously. The lost power at the photo diode is thereby accounted for the measurements with the power meter to obtain accurate values.

## 3. Coupling stability

In order to obtain the correct shape of the beam propagation within the cavity, i.e. mode matching, the position of the two lenses within the laser path have to be aligned thoroughly. Furthermore, the influence of optical components within the laser path needs to be considered, since the refraction index of larger than unity impacts the beam propagation. This was performed by stepwise setting-up of the optical components and measuring the beam profile with a scanning-slit beam profiler. The required beam waist at the cavity focus could be confirmed [15] and with that the envisaged Gaussian beam propagation within the resonator. The final Gaussian beam has a diameter of 0.8 mm in the focus in the middle of the cavity and 1.2 mm at the mirror surfaces. Details on the mode matching can be found in [15].

For locking the longitudinal mode (laser wavelength) to the cavity resonance, the PDH feedback system is set into operation by thoroughly adjusting the multitude of feedback parameters. Only using the PZT channel, stable resonance locking could be achieved for 1–2 min, after which thermal drifts beyond the tuning range of the PZT channel drive the cavity out of resonance and the coupling is lost.

In order to compensate for this drift, the second feedback channel is used, which continuously drives the slow 'thermal' channel. The result is to be seen in Fig. 3. The cavity transmission and the error signal from the PDH system are shown together with the signals from the feedback system, i.e. the PZT voltage applied via the fast channel and the drift compensation voltage from the slow channel, corresponding to the variation of the Nd:YAG crystal temperature (1 °C/V). Next to the figure, a photograph of the laser beam within the cavity is shown, representative for the entire time. The actually measured signals have a length of two minutes and are recorded every ten minutes. For the figure, the signals have been averaged over these two minutes and the

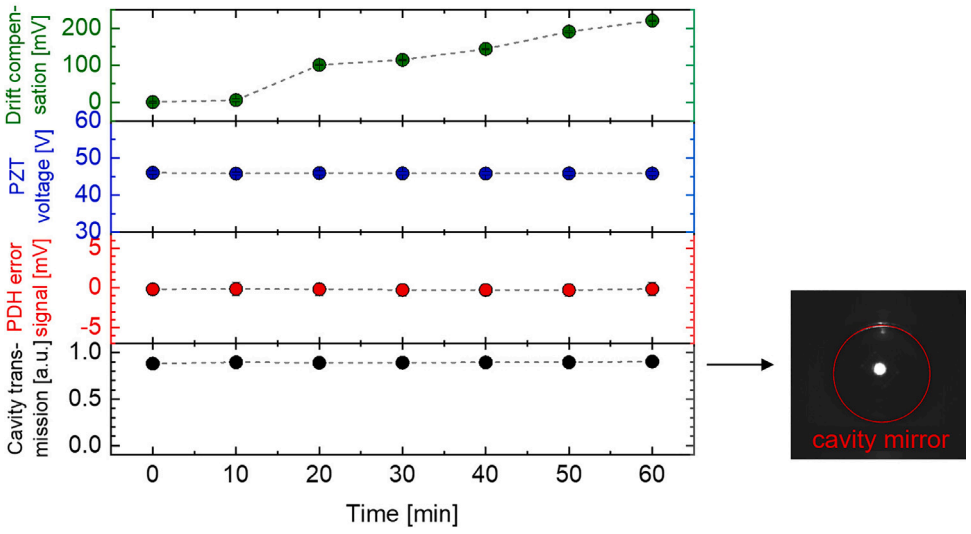


**Fig. 3.** Signals during stable cw coupling in resonance over 1 h using a fast feedback channel and a slow drift compensation channel. The photograph shows the coupled mode recorded with the camera behind the output mirror.

standard deviation within this time span is given as error bars, which are mostly smaller than the symbol size.

It can be seen that the cavity transmission stays constant and the error signal for the feedback system stays at zero. This means that the cavity is driven at optimal conditions, i.e. at resonance. The coupled mode during the entire time is Gaussian, as can be seen at the circular shape in the photograph. The PZT channel does not show any variation during this time, which means that it can fully operate within its envisaged regime, i.e. compensation of short-time vibrations that are not to be seen at the shown time scales. The drift compensation now shows an increase by 200 mV, which relates to an increase of the laser crystal temperature by 0.2 °C which in turn means a change of the laser wavelength by 2.5 pm within an hour.

This result thus illustrates the stable cw amplification of a Gaussian beam by an external cavity. Even to the end of this time, no signs for an imminent loss of stability were given, i.e. the coupling could have been easily realized for longer times. A limitation could be given by the continuous increase of the Nd:YAG crystal temperature, by which a mode hop of the seed laser, i.e. an almost instantaneous change of the laser frequency, can be reached after some time. Since this frequency change cannot be compensated and would lead to a loss of coupling, it needs to be avoided. If a continuous linear drift is extrapolated, this would happen after about 4.5 h in total in the current configuration. However, since the drift is supposed to be of thermal nature, equilibration is to be expected leading to even longer coupling times. Beyond that, countermeasures against the thermal drift like a system presented in [14] or piezo-actuators acting on the mirrors themselves to slowly adapt the resonance frequency to compensate the thermal drift could be thought of.

In the status presented in Fig. 3, the absolute amplification was relatively low, namely at 376 (compare to the targeted value of up to $10^4$). It turned out, that this came from degraded mirror surfaces: using a pulsed cavity-ringdown system (CRDS) in parallel to the cw high-power laser, the reflectivity could be absolutely measured and it was below 99.98%. The reason for this degradation from the initial 99.995% was the application of the mirrors in a CRDS system to measure negative hydrogen ions at hydrogen plasmas before their usage in the current system. The degradation behaviour of high-reflective mirrors under such conditions is described in [18] and is expected to arise from the VUV radiation of the hydrogen plasma. Hence, for further studies on the achievable amplification, fresh mirrors with their nominal reflectivity have been installed afterwards and are used for the following investigations.

## 4. Amplification

In order to determine the internal amplification of the cavity, first the mathematical basis is formulated below and correlated to the experimentally accessible parameters from the diagnostics (Section 4.1). Particular focus is laid on the difference between 'resonant systems', i.e. coherent systems driven in resonance, and 'non-resonant systems', e.g. pulsed systems that are inherently in-coherent from pulse to pulse, which brings out the implicit difference in the maximally achievable gain factor. The obtained results of the current setup are presented in Section 4.2.

### 4.1. Mathematics and diagnostics

In the following, a linear two-mirror cavity is considered in which the laser enters through one of the cavity mirrors. An illustrative depiction of the used variables is given in Fig. 4. The intensity or power density of the laser field within the cavity $P_{\mathrm{cav}}$ is proportional to $|\sum_n \vec{E}_n|^2$, where $\vec{E}_n$ is the electric field after the $n$th roundtrip ($n \to \infty$) within the cavity.[3] It is related to the $n$th power by $P_n \propto |\vec{E}_n|^2$, which in turn depends on the roundtrip-attenuation $\theta$ via $P_n = P_0\theta^n$, with the initial power $P_0$ before the first roundtrip and $\theta$ given by

$$\theta = R^{*2}(1 - L) \ , \tag{2}$$

where $R^*$ is the (measured[4]) reflectivity of the cavity mirrors and $L$ the roundtrip losses that need to be minimized in experiment. To evaluate the square of the absolute of the electric fields sum, two extreme cases are distinguished:

- In resonance, the term $\vec{E}_n\vec{E}_{n+1}$ yields $|\vec{E}_n||\vec{E}_{n+1}|$ and thus:

$$\left|\sum_n \vec{E}_n\right|^2 = \left(\sum_n |\vec{E}_n|\right)^2 \propto \left(\sum_n \sqrt{P_0\theta^n}\right)^2 \ . \tag{3}$$

  Using the geometric series leads to:

$$\left(\sum_n \sqrt{P_0\theta^n}\right)^2 = \left(\sqrt{P_0}\frac{1}{1-\sqrt{\theta}}\right)^2 = P_0\frac{1}{\left(1-\sqrt{\theta}\right)^2} \ . \tag{4}$$

[3] $P_{\mathrm{cav}} \equiv P$ in Eq. (1).

[4] Measurements are performed by CRDS and thus inherently include short-time losses of time scales below about 1 ms. Hence, the measured value is typically smaller than the actual one, which is considered by using the asterisk $*$ added to the $R$.

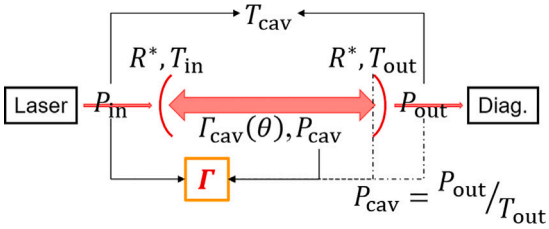


**Fig. 4.** Illustration of the defined variables to describe the amplification by the cavity.

- For the second case it is considered that the cavity is filled with an infinite amount of pulses from a highly repetitive pulsed laser. In this case, representative for 'non-resonant systems', the electric fields are not coherent with each other and all the components of $\vec{E}_n \vec{E}_{n+1}$ will cancel out due to randomly distributed phases between the vectors. This yields:

$$\left|\sum_n \vec{E}_n\right|^2 = \sum_n \left(|\vec{E}_n|^2\right) \propto \sum_n P_0 \theta^n = P_0 \frac{1}{1-\theta} \,. \tag{5}$$

The fraction to the end of both equations is abbreviated by the intra-cavity amplification $\Gamma_{cav}$ and the initial intra-cavity power $P_0$ is related to the input power $P_{in}$ by the transmission $T_{in}$ through the input mirror, which, for the resonant case, finally gives

$$P_{cav} = P_0 \frac{1}{\left(1-\sqrt{\theta}\right)^2} = P_{in} T_{in} \Gamma_{cav}(\theta) =: P_{in} \Gamma(\theta) \,, \tag{6}$$

where in the last step the *amplification of the cavity* in the current sense is defined as the ratio of the intra-cavity power to the input power.

Assuming negligible absorption within the mirror material ($\Rightarrow T_{in} = 1 - R$) and no roundtrip losses ($L = 0 \Rightarrow \theta = R^2$), an upper limit for the amplification in the above-mentioned cases (4) and (5) can be given:

$$\Gamma = T_{in}\Gamma_{cav} = \begin{cases} \text{in resonance} & \frac{1-R}{(1-\sqrt{R^2})^2} = \frac{1}{1-R} > 1 \;\forall\, R \\ \text{non-coherent} & \frac{1-R}{1-R^2} = \frac{1}{1+R} < 1 \;\forall\, R \end{cases} \tag{7}$$

This explains the advantage of using resonant amplification instead of simply 'adding up non-coherent wave packages', as in the latter case no net gain can ever be obtained as long as the laser is entering the resonator through one of the cavity mirrors with reflectivity $R$.

Measuring the amplification experimentally requires a further step, since the intra-cavity power is not accessible directly. Thus, the transmitted power $P_{out}$ through the output mirror is used and related to $P_{cav}$ by the output mirror transmission $T_{out}$:

$$P_{cav} = \frac{P_{out}}{T_{out}} \quad \Rightarrow \quad \Gamma = \frac{P_{out}}{T_{out} P_{in}} =: \frac{T_{cav}}{T_{out}} \,. \tag{8}$$

This leads to the definition of the cavity transmission $T_{cav} = P_{out}/P_{in}$, which is the actual value used to characterize the experimentally achieved performance of the cavity, since it is directly measured during operation with the calibrated power meter behind the cavity ($P_{out}$). $P_{in}$ is measured with the calibrated power meter in the side arm of the PDH system (see Fig. 2): it detects the reflected power from the cavity and thus, the measured value only resembles $P_{in}$ before and after coupling, since during coupling (i.e. in resonance) part of the total power is transmitted through the cavity and the measured value decreases consequently. Losses at the optical components between the cavity and the actual measurement position of the power meters ($P_{in}$ and $P_{out}$) are taken into account by a scaling factor determined beforehand. This procedure also confirmed the applicability of measuring $P_{in}$ in the side arm when the cavity is not driven in resonance.

### 4.2. Results

Fig. 5 shows the theoretically achievable cavity transmission (linked to the amplification via Eq. (8)) for the current setup as the full line (disregarding the open points at first) depending on the roundtrip losses $L$, calculated via Eqs. (8), (6) and (2), i.e.

$$T_{cav} = T_{in}\Gamma_{cav}(\theta)T_{out} = \frac{T_{in}T_{out}}{\left(1-\sqrt{R^{*2}(1-L)}\right)^2} \,. \tag{9}$$

Given in Section 2, the theoretical maximal amplification for $L = 0$ is at 15'600 or a cavity transmission of 0.61. For $L = 10^{-6} = 1$ ppm, $T_{cav}$ decreases only negligibly to 0.60, the amplification being ≈15'300. With increasing $L$ the amplification drops down to 129 ($T_{cav} = 0.005$) for $L = 1000$ ppm.

Realistic experimentally achievable cavity losses might be in the range of 10 to 100 ppm, which would yield amplifications in the range of 3'900 to 12'900. This range is approached by thorough manual alignment of all optical components and optimizing the feedback parameters. The result is given in the figure by the alphabetically enumerated open points (A → D), representing specific statuses during this procedure. Only the PZT channel was used for this campaign yielding only some minutes of coupling, but no indications were given that would contradict longer coupling using also the thermal channel as shown in Section 3.

Starting from an amplification of about 1'000 (A) the current status gives a maximal experimentally achieved amplification of 6'982 ± 1'054 (D). In this status the transmitted power was 65.1 mW (± 4%) at an input power of 238.9 mW (± 3%), giving a cavity transmission of 0.27 (± 7%). The intra-cavity power hence yields $P_{cav} = 1.67$ kW (± 12%[5]) and roundtrip losses account to $L = 49.5 \pm 11.2$ ppm. The intra-cavity amplification in this status gives $\Gamma_{cav} \approx 1.8 \times 10^8$, i.e. the laser intensity is multiplied 180 million times within the resonator (coming from 13'400 coherent superpositions of the laser beam) to compensate the $(39\,\text{ppm})^2$ transmission through the mirrors. This achievement can be seen as a successful implementation of a cw-driven cavity with high amplification, albeit the performance curve indicates that even higher values should be achievable by further decreasing the roundtrip losses.

However, the coupled mode for these high amplifications is not yet purely the envisaged Gaussian mode, having the highest power density required for neutralization of an ion beam. While status A and B are still Gaussian ($TEM_{00}$), C already has significant contributions from $TEM_{01}$ and $TEM_{10}$: those modes can accumulate powers up to 500 W each, while slightly more than 1 kW is left for the Gaussian mode. The complication of this issue is that different transversal modes typically have different resonant frequencies (in particular for the lower orders 00, 01, 02, etc.), which means that only one of them can be stably locked at a time, while the remaining power that could be coupled to another mode at another frequency is lost. In the current case, the 1 kW coupled Gaussian mode is plotted for point C in the figure.

For the highest achieved amplification (D) the mode structure is given in the photograph, showing pretty high orders next to the Gaussian mode. Those high orders can have the same resonant frequency [19] and are thus coupled simultaneously and lead to the high coupled power of 1.7 kW. However, the power density distribution is still unfavourable for laser neutralization. Further decreasing the roundtrip losses will thus certainly need to include optimizing the transversal mode, i.e. the mode matching, in view of laser neutralization.

[5] The in-house determined transmission $T_{out}$ has an error of ± 8% due to the accuracies of 3% and 4% of the applied power meters and 1% statistical error of a multitude of transmission measurements.

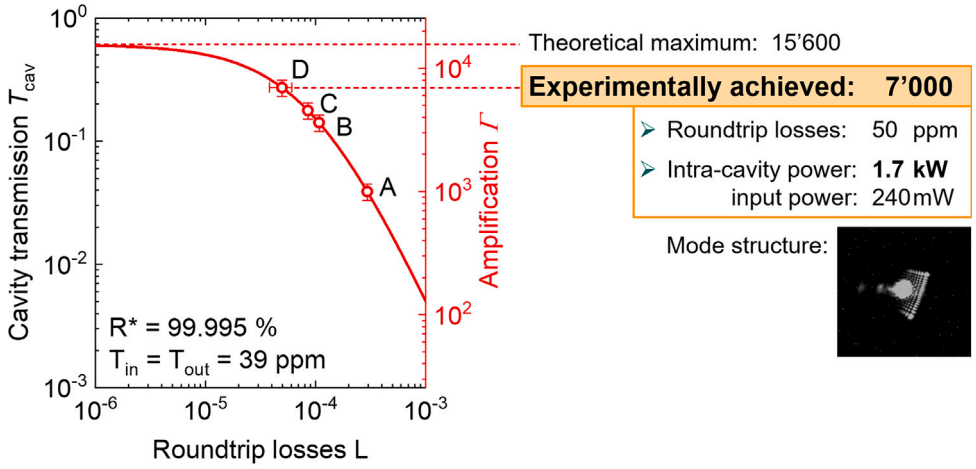


**Fig. 5.** Performance plot of the current cw-driven cavity. Cavity transmission and absolute amplification are linked via Eq. (8). The full line represents the theoretical dependence after Eq. (9), the experimentally achieved statuses are plotted with open points A-D, the alphabetical order denotes the chronology. The photograph shows the coupled mode for point D.

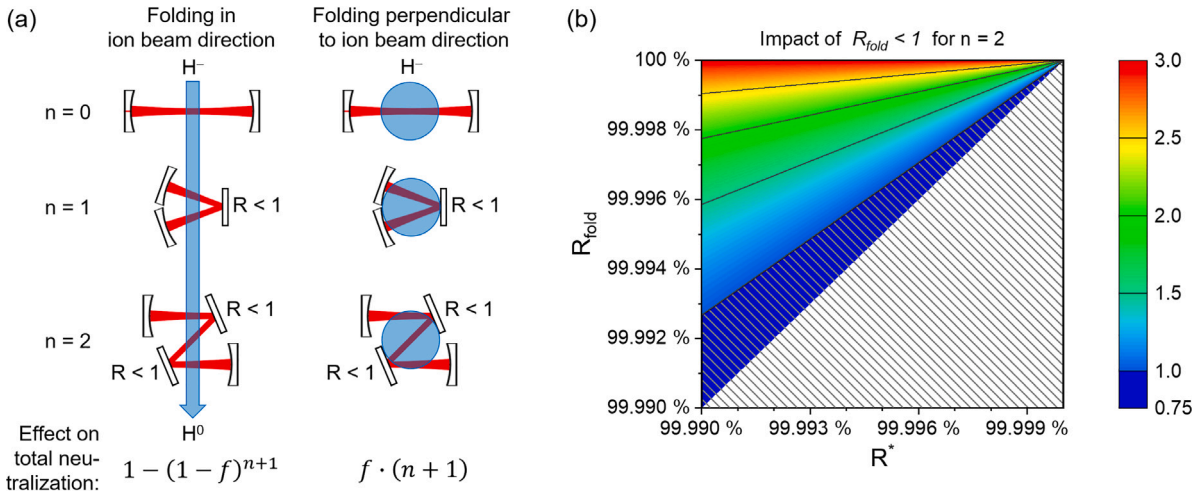


**Fig. 6.** (a) Illustration of folding geometries: (i) in ion beam direction and (ii) perpendicular to it (ion beam propagation is into or out of the drawing plane). (b) Influence of the folding mirrors' reflectivity on the achievable neutralization upon double folding perpendicular to the ion beam axis (geometry (ii) from part (a)).

## 5. Application to negative ion beams

An option to test the system for actual neutralization of an ion beam would be to apply it to the Batman Upgrade facility (BUG) [20]. Design integration studies have been performed in which masking of the multitude of extraction apertures as well as beam divergence between extraction and the possible position of the optical cavity was considered. The following description focuses on the achievable performance using the status of the optical setup presented above and is to be seen as an upper limit. Detailed design of the real neutralizer system would be part of a future publication dealing with the implementation itself.

In order to obtain a beam sheet with minimal extension perpendicular to the laser beam, four of the five aperture columns of the plasma grid (PG) are covered, leaving 1 × 14 apertures for extraction with 14 mm diameter each. The optical neutralizer cavity could be installed 1 m downstream the extraction system. Assuming a beam divergence of 1°, the beam will increase to a size of about 29 × 3 cm (due to overlapping apertures; equiv. to $h \times w$ in Fig. 1(a)). Using the laser beam diameter of in average 1 mm (see Section 3), 3.25% of the ion beam would be covered.

Tests could be performed at a total extraction and acceleration voltage of 20 kV, giving a 20 keV ion beam. Using Eq. (1) with the achieved amplification of 7'000 and an input power of 6.2 W (the maximum power level reaching the optical cavity after transmission trough all the optical components), 34% neutralization efficiency within the laser beam could be achieved.

Taking into account the non-neutralized part of the ion beam outside the laser beam (covering fraction only 3.25%), in total about 1% of the negative ion beam could be neutralized in the present status. This small fraction poses the question about detecting such a small neutralization and measures like folding the laser beam or using a beam scraper for the ion beam need to be discussed.

For folding the cavity, two options exist depending on the geometry of the folded arms in relation to the ion beam, illustrated in Fig. 6(a):

- (i) Folding the cavity in beam propagation axis, the same part of the beam is neutralized again, which leads to a higher total neutralization degree after $1-(1-f)^{n+1}$, where $f$ is the neutralization degree for single beam-laser-interaction and $n$ is the folding order.
- (ii) Folding the cavity perpendicular to the beam propagation axis, a larger section of the ion beam is covered by the laser and the neutralized fraction of the ion beam increases accordingly linearly with $n$.

The decision depends on the actual geometry of ion and laser beam, and for BUG where the laser beam is much smaller than the ion beam,

option (ii) is much more effective. However, since folding the cavity is done by mirrors with a reflectivity of below unity, the influence of these additional lossy surfaces on the amplification of the cavity need to be taken into account. Considering the folding mirrors' reflectivity $R_{\mathrm{fold}}$ for the roundtrip attenuation yields:

$$\theta_{\mathrm{fold}} = R^{*2} R_{\mathrm{fold}}^{n} (1 - L) \ . \tag{10}$$

The impact can be seen in Fig. 6(b). Using Eq. (6) without losses, the achievable amplification is calculated for different reflectivities of the cavity and folding mirrors for double folding ($n = 2$) and multiplied by three to consider the increased neutralization. The result is divided by the calculation without folding, i.e. $n = 0$.

It can be seen that for non-lossy folding mirrors ($R_{\mathrm{fold}} = 1$), folding would give the expected three-times higher neutralization. On the other hand, folding with the same reflectivity as the cavity mirrors would always lead to 25% loss of total neutralization. This is due to the fact that the loss due to the folding mirrors is already 75%, i.e. down to 25% of the initial value without folding. Multiplying by three still yields only 75% of the initial value. Hence, the effect of folding can easily be overcompensated by the additional lossy surfaces. For the current setup with a cavity mirror reflectivity of 99.995%, the folding mirrors reflectivity would need to be larger than 99.9964% to have a positive impact of folding. Considering the additional complexity of such a folded cavity, in particular in view of the more difficile alignment and more possibly degradable surfaces during long-time operation, it needs to be carefully assessed if folding is an advantageous possibility to increase neutralization efficiency.

## 6. Conclusions

In order to increase the neutralization efficiency for negative hydrogen ion beams w.r.t. a gas neutralizer, laser neutralization by employing the photodetachment process is discussed. The required high optical powers need to be delivered by amplifying a seed laser for reasonable application and the resonant external enhancement cavity concept, where the ion beam will be within an optical resonator continuously driven by the coupled seed laser, is studied here.

It is shown, that with a sophisticated 2-channel feedback system the laser can stably be coupled in the envisaged Gaussian mode for more than 1 h, albeit the performance of the cavity in terms of amplification was not optimized. The mathematical formalism for the amplification within the resonator confirmed the unsurpassed performance of resonance coupling in contrast to non-resonant systems. Experimental results revealed amplifications of up to 7'000, which is the proof-of-concept for application relevant amplifications. Optimization steps include the further decrease of roundtrip losses as well as the improvement of the transversal mode towards a purely Gaussian propagation with the cavity.

In view of application of the current system to an actual ion beam, an assessment of the achievable neutralization was done for the Batman Upgrade ion beam: even if the actual neutralization within the interaction region is already at 34%, the small covered fraction of the ion beam by the laser beam leads to only 1% neutralized fraction of the ion beam in the current status, and is seen as not reasonable at the moment due to the difficulties of detecting this small fraction. Furthermore, it was shown that folding the cavity, for which several reasons might exist (increasing neutralization efficiency, increasing laser-beam-ion-beam interaction zone, shortening of the cavity length, ...), can easily overcompensate the envisaged effect due to the implementation of further lossy surfaces.

In conclusion, no 'show-stoppers' were identified for laser neutralization of negative ion beams and stable cw-coupling of a laser to a high-finesse cavity driven in Gaussian mode as well as application relevant amplifications could be shown experimentally.

## CRediT authorship contribution statement

**R. Friedl:** Writing – original draft, Visualization, Validation, Supervision, Software, Methodology, Investigation, Formal analysis, Data curation, Conceptualization. **R. Borkenhagen:** Visualization, Investigation, Formal analysis, Data curation. **U. Fantz:** Writing – review & editing, Supervision, Project administration, Funding acquisition, Conceptualization.

## Declaration of competing interest

The authors declare that they have no known competing financial interests or personal relationships that could have appeared to influence the work reported in this paper.

## Acknowledgements

This work has been carried out within the framework of the EUROfusion Consortium, funded by the European Union via the Euratom Research and Training Programme (Grant Agreement No 101052200 — EUROfusion). Views and opinions expressed are however those of the author(s) only and do not necessarily reflect those of the European Union or the European Commission. Neither the European Union nor the European Commission can be held responsible for them.

## Data availability

Data will be made available on request.

## References

[1] M.Q. Tran, et al., Fusion Eng. Des. 180 (2022) 113159.
[2] J.H. Fink, A.M. Frank, 1979, US Patent 4, 140, 577.
[3] J.H. Fink, AIP Conf. Proc., Vol. 111, 1984, p. 547.
[4] T. Inoue, et al., Fusion Eng. Des. 81 (2006) 1291.
[5] W. Chaibi, C. Blondel, L. Cabaret, C. Delsart, C. Drag, A. Simonin, AIP Conf. Proc., Vol. 1097, 2009, p. 385.
[6] M. Kovari, B. Crowley, Fusion Eng. Des. 85 (2010) 745.
[7] A. Simonin, C. Blondel, W. Chaibi, C. Dechelle, C. Drag, E. Villedieu, Nucl. Fusion 61 (2021) 046003.
[8] M. Genevriez, X. Urbain, Phys. Rev. A 91 (2015) 033403.
[9] K.H. Berkner, R.V. Pyle, J.W. Stearns, Nucl. Fusion 15 (1975) 249.
[10] H. Kreckel, et al., Science 329 (2010) 69.
[11] S.S. Popov, et al., Nucl. Fusion 58 (2018) 096016.
[12] A. Fassina, D. Fiorucci, L. Giudicotti, P. Vincenzi, J. Instrum. 15 (2020) C02031.
[13] D. Bresteau, C. Blondel, C. Drag, Rev. Sci. Instrum. 88 (2017) 113103.
[14] D. Fiorucci, J. Feng, M. Pichot, W. Chaibi, AIP Conf. Proc., Vol. 1655, 2015, 050010.
[15] R. Friedl, F. Merk, C. Hopf, U. Fantz, AIP Conf. Proc., Vol. 2011, 2018, 060006.
[16] A. O'Keefe, D. Deacon, Rev. Sci. Instrum. 59 (1988) 2544.
[17] R.W.P. Drever, J.L. Hall, F.V. Kowalski, J. Hough, G.M. Ford, A.J. Munley, H. Ward, Appl. Phys. B 31 (1983) 97.
[18] D. Rauner, U. Kurutz, U. Fantz, AIP Conf. Proc., Vol. 1655, 2015, 020017.
[19] G.O. Harding, Tingye Li, J. Appl. Phys. 35 (1964) 475.
[20] U. Fantz, et al., Fusion Eng. Des. 146 (2019) 212.